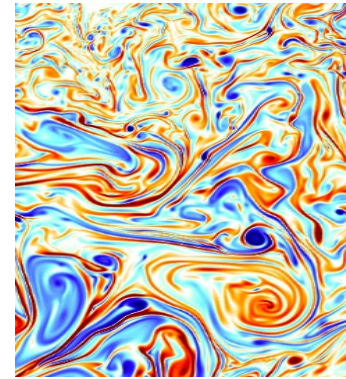
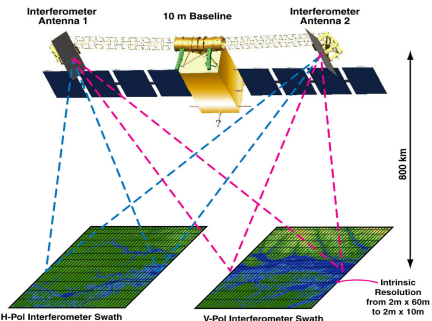


# “Ocean Turbulence from SPACE”

Patrice Klein (Caltech/JPL/Ifremer)

**(XVI) – Geostrophic turbulence (c):**  
Inverse energy cascade and direct enstrophy (potential) cascade



## Geostrophic (3-D) turbulence

$$\frac{dq}{dt} + \beta \psi_x = 0 \quad (5) \quad \text{with } q = \Delta \psi + \frac{\partial [f^2 \partial \psi]}{\partial z [N^2 \partial z]} \quad (5)$$

$q$  is the QG potential vorticity.

$\psi$  is obtained from  $q$  by inverting a 3-D elliptic operator (6), using appropriate boundary conditions.

The problem to solve is:

$$\Delta \psi + \frac{\partial [f^2 \partial \psi]}{\partial z [N^2 \partial z]} = q.$$

$$\text{with } \left. \frac{\partial \psi}{\partial z} \right|_{z=0} = -\frac{q}{\rho_0 f_0} \quad \rho' \Big|_{z=0} \quad \text{and} \quad \left. \frac{\partial \psi}{\partial z} \right|_{z=-H} = 0.$$

$$\left. \begin{array}{l} \\ \end{array} \right\} \quad (7).$$

Only the time evolution of  $q(t)$  [eq. 5] and  $\rho' \Big|_{z=0}^{(t)}$  [eq. 2 with  $w=0$ ] are needed!

We assume  $\rho'(t, z=0) = 0$ !

# Understanding the inverse energy cascade and direct enstrophy cascade (i.e. non-linear scale interactions) requires to move to the spectral (3-D) space

## 1) Horizontal dimensions:

It is convenient to express variables ( $\psi$ ) in terms of double Fourier integral:

$$\hat{\psi}(x, y) = \frac{1}{2\pi} \iint_{kl} \tilde{\psi}(k, l) e^{ikx + ly} dk dl,$$

with  $k$  and  $l$  respectively the zonal and meridional wavenumbers.

If  $\psi$  is the stream function [ $u = -\psi_y$ ,  $v = \psi_x$ ] we get:

$$|\tilde{u}(k, l)|^2 + |\tilde{v}(k, l)|^2 = (k^2 + l^2) |\tilde{\psi}(k, l)|^2$$

$$|\tilde{\zeta}(k, l)|^2 = - (k^2 + l^2) |\tilde{\psi}(k, l)|^2 \quad \text{with } \zeta = v_x - u_y.$$

We will use:

$$E(k) = \iint_{kl} [(|\tilde{u}(k, l)|^2 + |\tilde{v}(k, l)|^2) dk dl \quad \text{with } k^2 + l^2 = k^2]$$

$$Z(k) = \iint_{kl} |\tilde{\zeta}(k, l)|^2 dk dl \quad \text{with } k^2 + l^2 = k^2$$

## 2) Vertical dimension using normal modes:

Normal modes are obtained by solving the Sturm-Liouville equation (after [J. Sturm](#) (1803–1855) and [J. Liouville](#) (1809–1882)):

$$\frac{d}{dz} \frac{f^2}{N^2} \frac{dF_m}{dz} = - \lambda_m^2 F_m.$$

with  $dF_m/dz = 0$  at  $z=0, -H$ .

$F_m$  is the eigenfunction and  $\lambda_m^2$  the eigenvalue (or the vertical wavenumber) associated with mode  $m$ .

Modes are orthonormal :

$$\int_{-H}^0 F_m \cdot F_n dz = \delta_{mn}$$

$$\Rightarrow \tilde{\Psi}_{k,l}(z) = \sum_{m=0}^{\infty} \tilde{\Psi}_{k,l,m} F_m(z).$$

$$\tilde{q}_{kl}(z) = \sum_{m=0}^{\infty} Q_{kl,m} F_m(z)$$

# Normal modes with a depth-dependent stratification $N^2(z)$ :

an example (see Smith & Vallis, JPO 2001)

Assume

$$\bar{\rho}(z) = 1 + \frac{(\rho_{\text{bot}} - \rho_{\text{surf}})}{\rho_0} \left[ 1 - e^{\frac{z}{\alpha}} \right]$$

with  $\alpha = \delta \cdot H$  ( $\delta < 1$ )

$$\Rightarrow N^2(z) = \frac{g(\rho_{\text{bot}} - \rho_{\text{surf}})}{\alpha \rho_0} e^{\frac{z}{\alpha}}$$

Using ( ) in ( ) leads to :

$$k_m \approx (R_d)^{-1} \frac{m\pi}{2} \quad \text{with } R_d = \frac{1}{f} \sqrt{g(\rho_{\text{bot}} - \rho_{\text{surf}})/\rho_0}$$

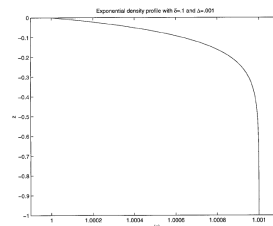
$$F_m(z) \approx \frac{\alpha}{H} e^{\frac{z}{\alpha}} \cos(m\pi e^{\frac{z}{\alpha}}) \quad m \geq 1$$

$$F_0(z) = 1$$

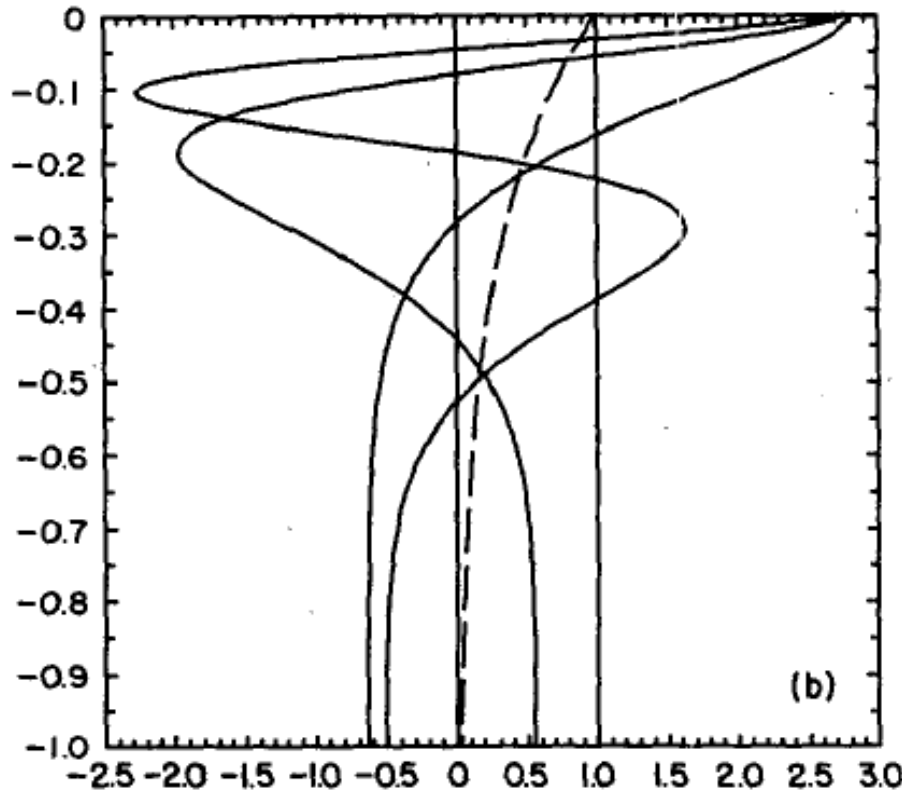
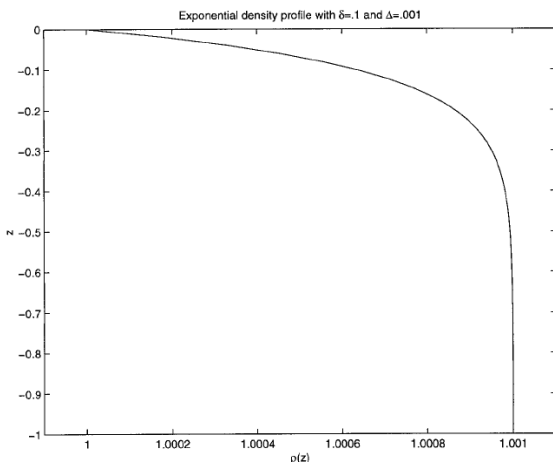
$$\Sigma_{mpq} = 2\left(\frac{\alpha}{H}\right)^{-1/2} \int_0^1 x^{1/2} \cos(m\pi x) \cos(p\pi x) \cos(q\pi x) dx$$

with  $x = e^{\frac{z}{\alpha}}$  and  $m, p, q \neq 0$ .

$$\Sigma_{mpq} = 1,0 \text{ if } m \cdot p \cdot q = 0.$$



# Comments on depth-dependent stratification ( $N^2(z)$ )



- The vertical wavenumbers are such that:  $\lambda_m = m \cdot \lambda_1$  ;
- Vertical normal modes are **surface intensified** (see figure);
- The interactions coefficients,  $\epsilon_{mpq}$ , **control the strength of the nonlinear mode couplings**.

## 3-D spectral PV equation

$$\hat{\Psi}_{k,l}(z) = \sum_{m=0}^{\infty} \hat{\Psi}_{k,l,m} F_m(z), \quad \hat{Q}_{k,l}(z) = \sum_{m=0}^{\infty} \hat{Q}_{k,l,m} F_m(z).$$

$$\frac{\partial}{\partial t} \hat{Q}_{k,l,m} + \sum_{pq} \epsilon_{mpq} \hat{J}_{k,l}(Y_p, Q_q) + ik\beta \hat{\Psi}_{k,l,m} = -\gamma(k^2 + l^2) \hat{Q}_{k,l,m}$$

with

$$\hat{Q}_{k,l,m} = -(k^2 + l^2 + \lambda_m^2) \hat{\Psi}_{k,l,m}.$$

$$\epsilon_{mpq} = \int_{-H}^0 F_m \cdot F_p \cdot F_q dz$$

The interactions coefficients,  $\epsilon_{mpq}$ , control the transfer between the different vertical modes.

## Conservation of total energy and potential enstrophy:

Two invariants as in 2-D turbulence.

$$E = \int_V \left[ |\nabla \psi|^2 + \frac{f^2}{N^2} \left| \frac{\partial \psi}{\partial z} \right|^2 \right] dv = \iint_{k,l,m} [k^2 + l^2 + l_m^2] |\tilde{\psi}_{k,l,m}|^2 dk dl dm$$

$$\mathcal{Z} = \int_V q^2 dv = \iint_{k,l,m} [k^2 + l^2 + l_m^2]^2 |\tilde{\psi}_{k,l,m}|^2 dk dl dm.$$

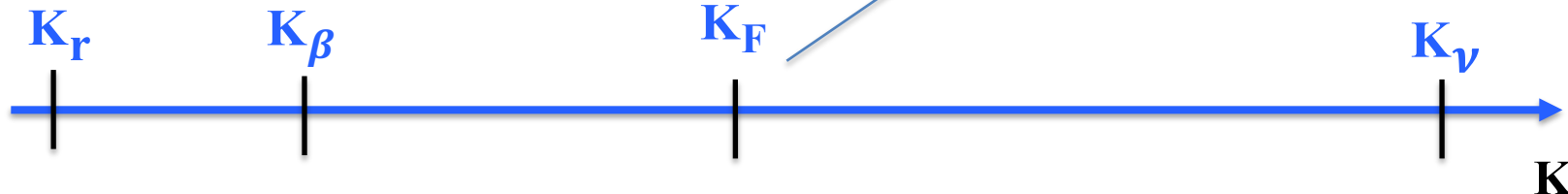
Given these two invariants, Charney (1971) showed that the only possibility is an inverse cascade of total energy and a direct cascade of potential enstrophy.

This emphasizes a formal analogy with the Kraichnan arguments for 2-D flows.

# Conservation of total energy and potential enstrophy:

$F$  is the forcing  
 $\beta$ -effect.  
 $\Omega$ : linear drag  
 $\nu$ : viscosity

$K_F$ .  
 $K_\beta$ .  
 $K_\Omega$ .  
 $K_\nu$



From Kraichnan (1957)'s arguments: the relative separation between  $K_r$ ,  $K_\beta$ ,  $K_F$  and  $K_\nu$  determines the dynamical regime that drive the non-linear interactions. Which allows to set up the spectral characteristics.

Following Kraichnan, Charney (1971) assumed that:

- For scales between  $K_F$  and  $K_\beta$  there is an inertial range with an inverse energy cascade.
- For scales between  $K_F$  and  $K_\nu$  there is an inertial range with a direct enstrophy cascade.

# Inertial range for the direct enstrophy cascade

Other assumptions (Charney JAS 1971):

- Turbulence is isotropic [no anisotropy of the energy and enstrophy in any of the three directions (horizontal and vertical)].
- The non-linear interactions are « local ».

Using the same dimensional considerations as in 2-D turbulence, he obtained:

Total energy

$$E(\mu) = C_e \eta^{2/3} \mu^{-3}$$

Potential enstrophy

$$\mathcal{Z}(\mu) = C_s \eta^{2/3} \mu^{-2} \quad \text{with } \mu^2 = k_x^2 + l_y^2 + l_m^2$$

Tracer

$$\mathcal{P}_c(\mu) = C_c \tilde{\eta}^{1/3} \chi \mu^{-1}$$

With  $\eta$  the enstrophy transfer function.

**These assumptions** (existence of two inertial ranges, homogeneity and isotropy, local non-linear interactions) **are questionable** and so have been tested in the QG framework (McWilliams'89, Hua and Haidvogel'86, Larichev and Held'95, Haynes & Anglade'97, Klein et al.'98, Smith & Vallis'02, Smith & Ferrari'09, Roullet et al.'12, Callies et al.16).

## Isotropy in geostrophic turbulence:

**It exists an aspect ratio between vertical and horizontal gradients**

The direct cascade of tracer (PV) variance is 3-D and therefore small vertical scales are readily produced. But because the cascade is expected to be isotropic in the wavenumber space ( $k, l, \lambda$ ), the small scales of tracer (PV) should maintain an aspect ratio of  $N/f$  throughout the inertial range. Such aspect ratio was later explored by Haynes & Anglade'97 using the followig arguments:

Let us consider a tracer  $C = C(x, y, z, t)$  conserved on a Lagrangian trajectory:

$$\frac{dC}{dt} = 0.$$

Tracer gradients are:

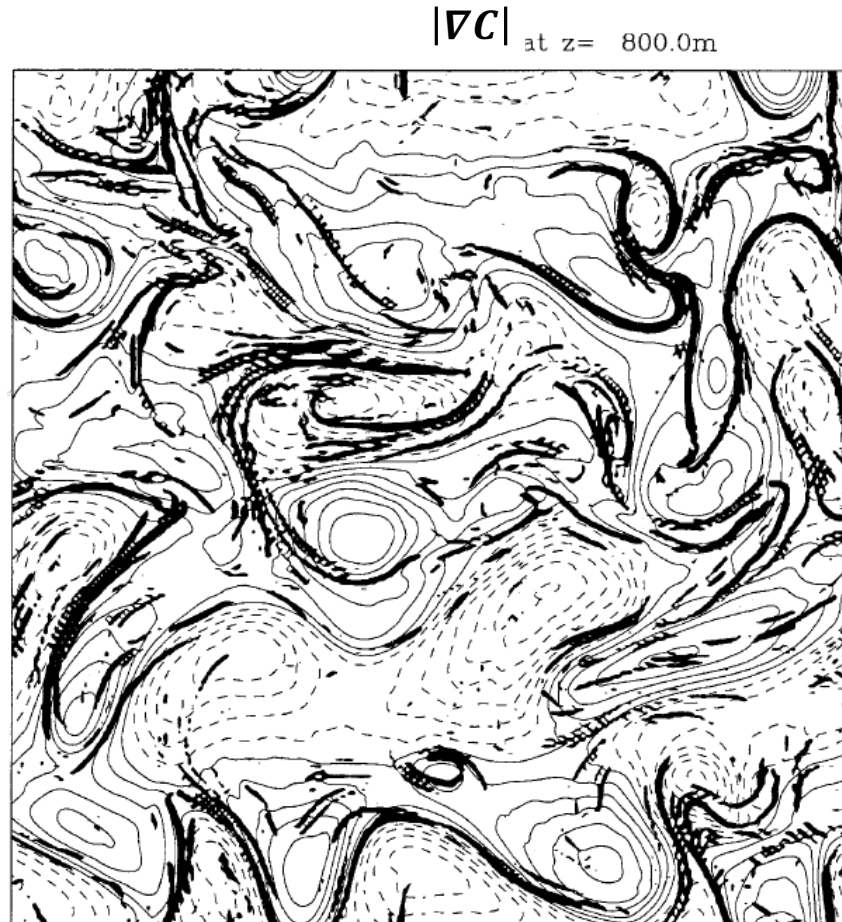
$$\frac{d}{dt} \begin{bmatrix} C_x \\ C_y \end{bmatrix} = - \begin{bmatrix} u_x & v_x \\ u_y & v_y \end{bmatrix} \begin{bmatrix} C_x \\ C_y \end{bmatrix}$$

$$\frac{d}{dt} C_z = - [u_z \quad v_z] \begin{bmatrix} C_x \\ C_y \end{bmatrix}$$

$C_x$  and  $C_y$  do not depend on  $C_z$  BUT  $C_z$  depends on  $C_x$  and  $C_y$  !

This suggests a relationship between vertical and horizontal scales of the tracer gradients

# Relationship between vertical and horizontal tracer gradients



Strong  $|\nabla C|$  are located around mesoscale eddies and in saddle areas where  $|\nabla \rho| \approx |U_z|$  is large.

What is the depth scale of these  $|\nabla C|$  patterns ?

# Relationship between vertical and horizontal tracer gradients

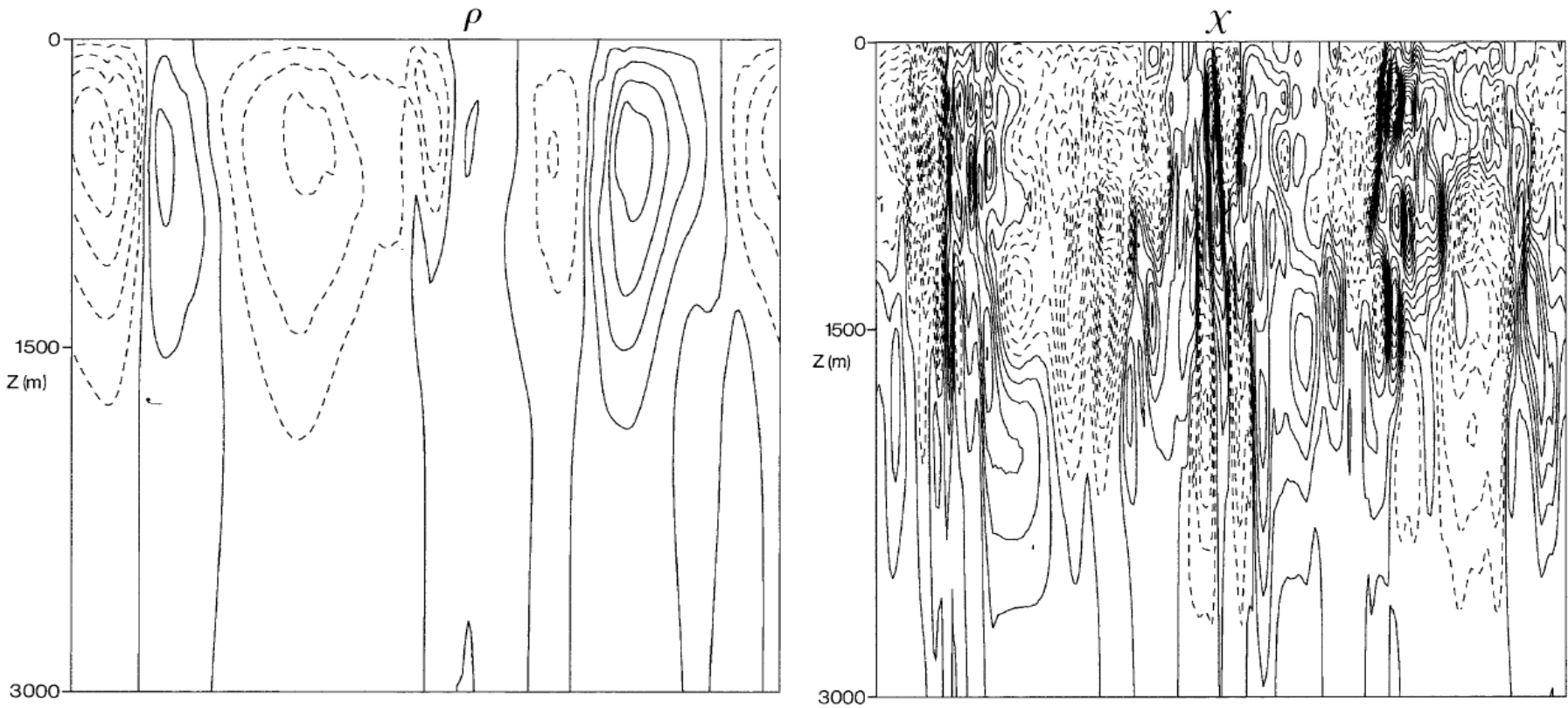


Figure 4. Vertical sections of  $\rho$  (a) and  $\chi$  (b) at the same time as Figure 2. The contour interval in nondimensional units is 1 for both fields. The isocontours range from -8 to 6 for  $\rho$  and from -14 to 14 for  $\chi$ . Solid and dashed lines respectively refer to positive and negative values.

The two fields,  $\rho$  and  $C$ , are nondimensionalized (same units) and the contour intervals are identical on both figures.

Horizontal gradients,  $|\nabla C|$ , have a small depth-scale compared with  $|\nabla \rho|$   
=> 3-D cascade

# Isotropy in geostrophic turbulence: aspect ratio between vertical and horizontal gradients

Let us consider a tracer  $C = C(x, y, z, t)$  conserved on a Lagrangian trajectory. In a strain dominated region we get:

$$\frac{d \nabla C}{dt} = -\sigma \nabla C \quad \frac{d C_z}{dt} = -\Lambda \nabla C.$$

with  $\sigma \approx [s_1^2 + s_2^2]^{1/2}$   $\Lambda = [u_z \ v_z]$

Assuming (for the sake of simplicity)  $\frac{d\Lambda}{dt} = \frac{d-\Lambda}{dt} \approx 0$ :

$$\Rightarrow \nabla C = \nabla C_0 e^{\sigma t} \quad C_z = \sigma^{-1} \Lambda \nabla C_0 e^{\sigma t}$$

Using  $C_g = \alpha \cdot \nabla C$

$$\Rightarrow \alpha = \frac{\Lambda}{\sigma}$$

$$\Rightarrow |\alpha|^2 = \frac{|C_z|^2}{|\nabla C|^2} \sim \frac{|\Lambda|^2}{\sigma^2}$$

A dimensional analysis indicates that:

$$\alpha^2 \approx N^2/f^2$$

The aspect ratio of the tracer gradients is given by the ratio of the shear ( $|U_z| \approx |\nabla \rho|$ ) acting across the tracer gradient and the strain rate ( $\sigma$ ). It scales as  $N/f$ . [see Haynes & Anglade'97, Klein et al.'98, Smith & Ferrari'09]

# Isotropy in geostrophic turbulence: aspect ratio between vertical and horizontal gradients

Smith & Ferrari JPO 2009

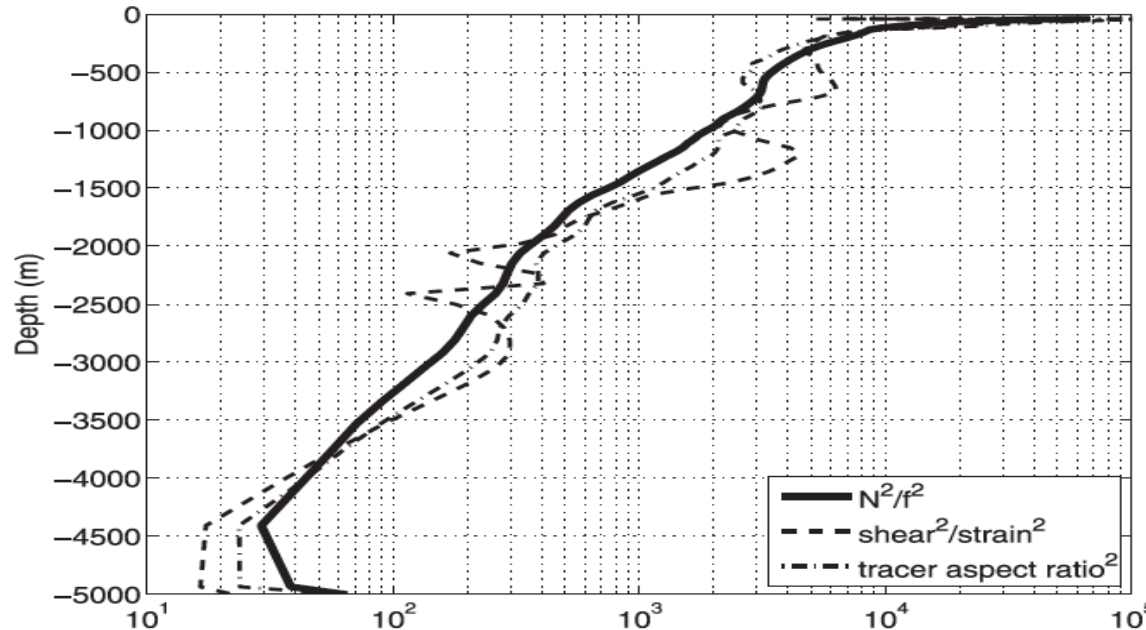


FIG. 13. Comparison of the squared Prandtl ratio  $(N/f)^2$  (solid), squared shear over strain  $|\overline{\mathbf{u}'_z}|^2/\sigma^2$  (dashed), and inverse squared tracer slope  $\overline{\phi_z^2}/|\nabla\phi|^2$  (dashed-dotted) for the central simulation. The strain is computed as  $\sigma^2 = \overline{(u'_y + v'_x)^2} + \overline{(u'_x - v'_y)^2}$ , where the overbar denotes both a time and horizontal spatial average.

The aspect ratio between vertical and horizontal scales is almost as  $N/f$ .

The isotropy assumption (no specific anisotropy in the horizontal direction relatively to the vertical one) seems to be verified (at least for scales smaller than  $K_F$ )

Consequences for the horizontal and vertical resolution in numerical models ...

## Isotropy of the tracer variance

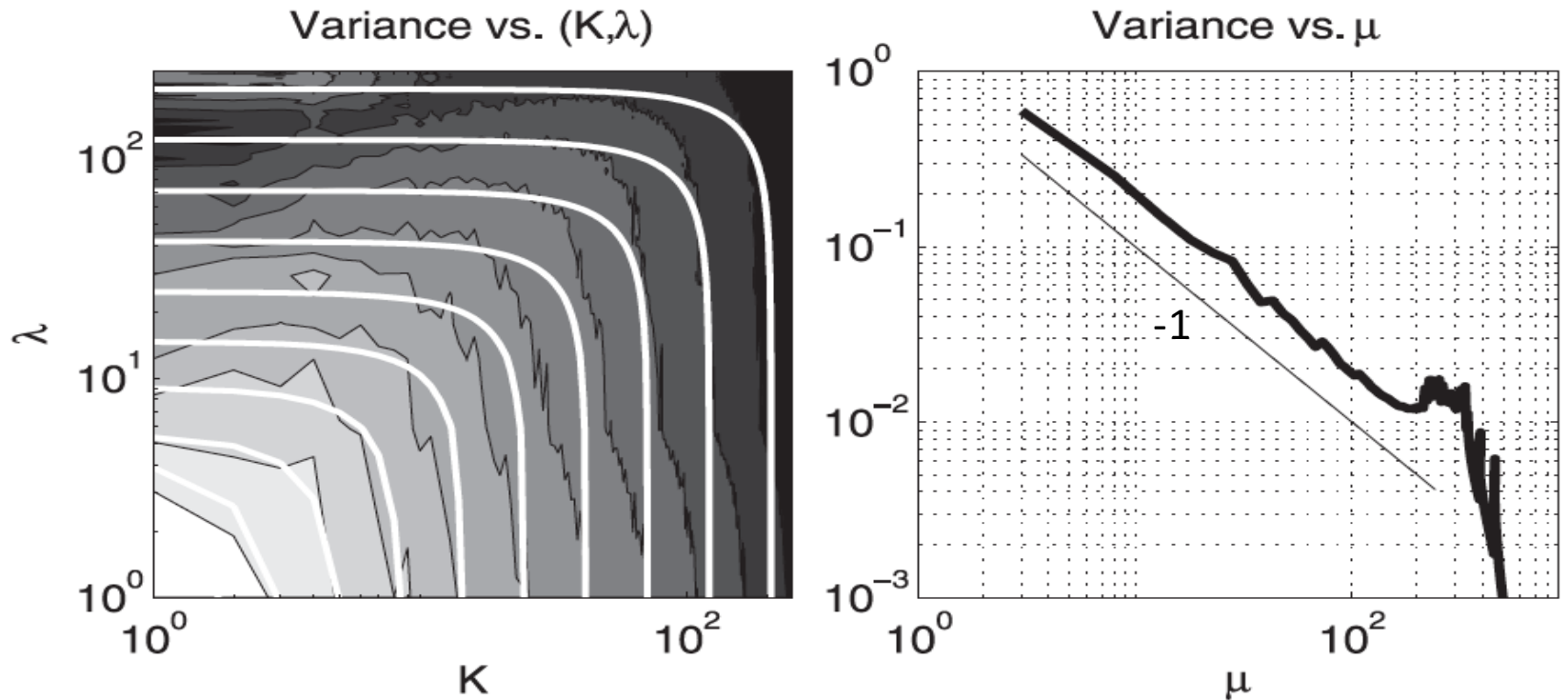


FIG. 11. (left) The spectrum of the logarithm of the tracer variance  $|\hat{\phi}_{k\lambda}|^2$ , integrated over horizontal spectral angle and plotted as a function of wavenumbers  $K$  and  $\lambda$  (nondimensionalized by  $2\pi/L_0$ , where  $L_0$  is the horizontal domain size), with logarithmic scaling. The white curves are isolines of  $\mu$ , and the tracer variance contours are logarithmically spaced between  $10^{-2}$  (lightest color) and  $10^{-5}$  (darkest color). (Right) The variance spectrum integrated over spherical shells, plotted as a function of  $\mu = \sqrt{K^2 + \lambda^2}$  (thick line), and a reference line proportional to  $\mu^{-1}$ . The

Smith & Ferrari JPO 2009

Such isotropy holds for the potential enstrophy. It should hold also for the total energy (see eqs. for the potential enstrophy and the total energy) ...

## Isotropy of the total energy

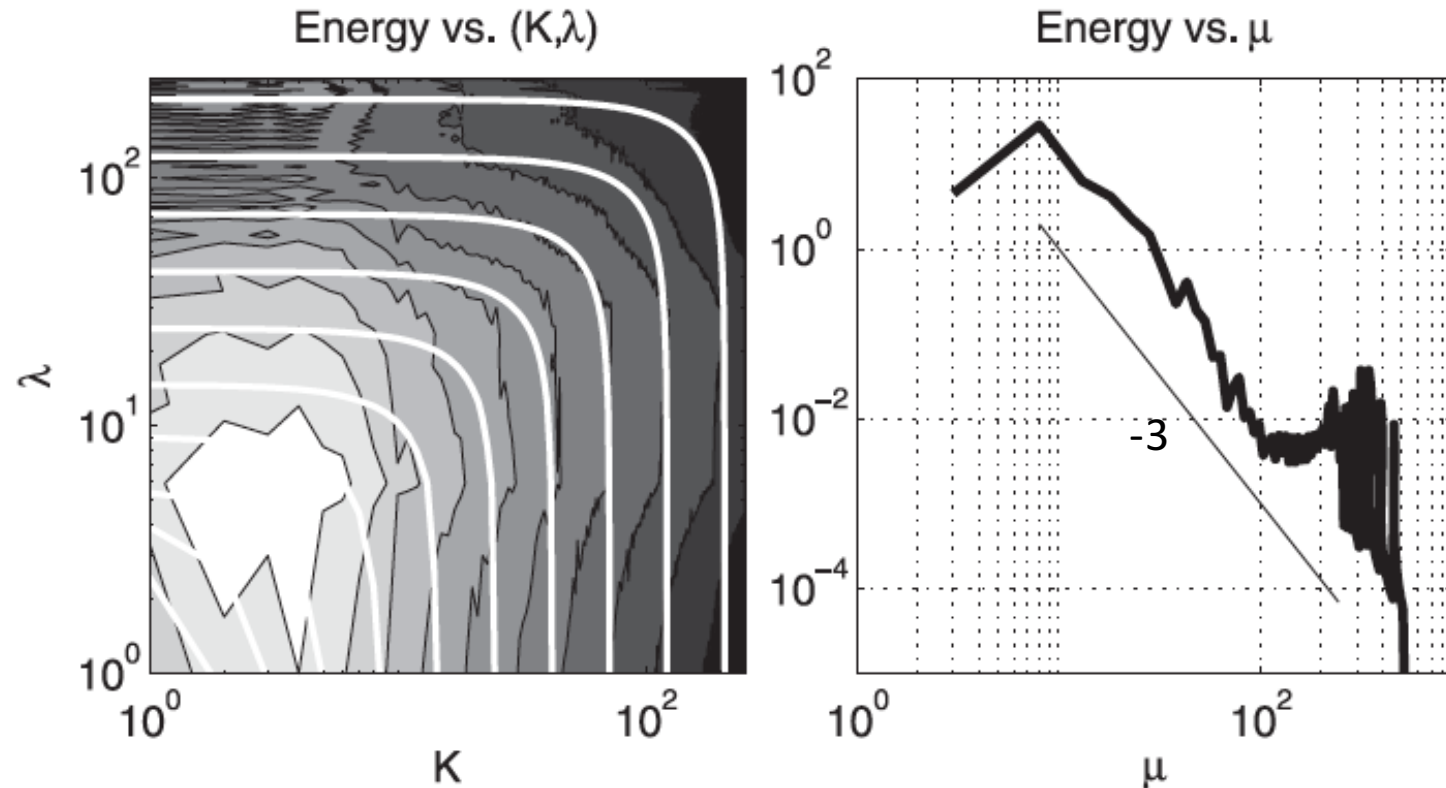


FIG. 12. Same as in Fig. 11, but for the nondimensional total energy  $E_{k\lambda} = \mu^2 |\hat{\psi}_{k\lambda}|^2$  of the central simulation. The energy contours are logarithmically spaced between 10 (lightest color) and  $10^{-6}$  (darkest color). The noise in the upper left is due to the effective high vertical mode forcing of the QGPV field, as a result of the complex structure of the mean QGPV gradient,  $\Gamma_q$ .

# Isotropy of the total energy

McWilliams JFM'89

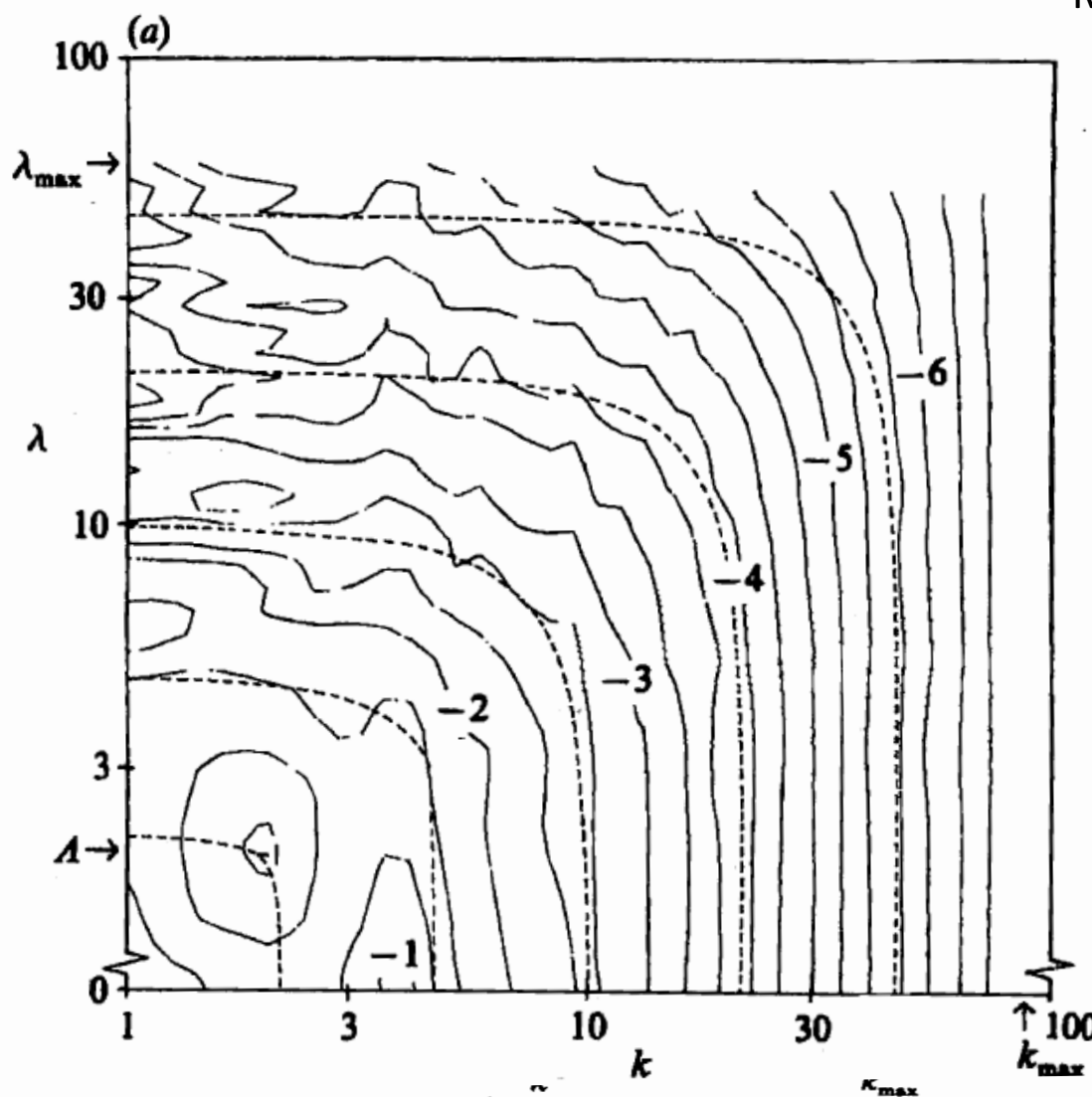
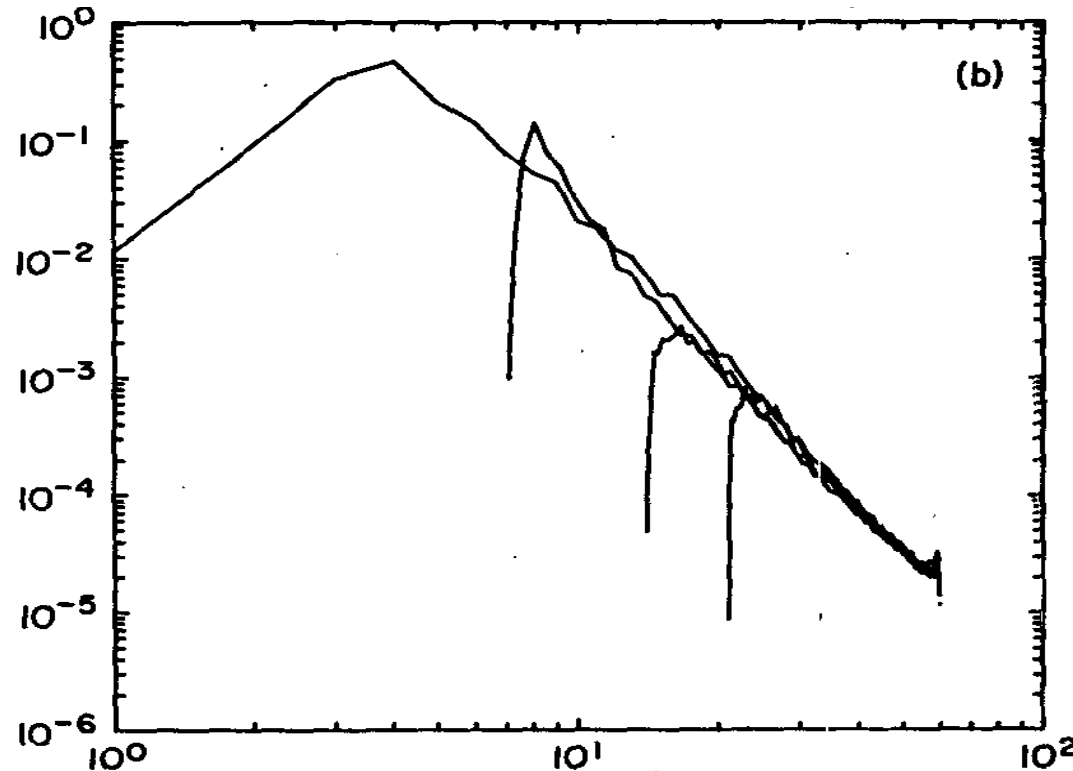


FIGURE 4.  $T_*(k, \lambda)/\cos \phi$  from (24) for solution A, averaged over  $6 \leq t \leq 8$ . Dashed lines are curves of constant  $\mu$ . (a)  $\log_{10}\{T_*/\cos \phi\}$ , with a contour interval of 0.33.

As anticipated by Charney (1971), the KE has the same form

$$KE(k, \lambda_m) = C_{KE} \eta^{2/3} \mu^{-3}$$

$$\mu^2 = k^2 + l^2 + \lambda_m^2$$



Hua & Haidvogel JAS86

FIG. 9. Modal components of the kinetic energy spectra for a constant Brunt-Vaisala stratification (run 3, Table 1). The components amplitudes decrease as the mode number goes from 0 to 3. Spectra are plotted as a function of (a) two-dimensional wavenumber and (b) three-dimensional wavenumber.

## Inertial range for the inverse energy cascade

Given these two invariants (total energy and potential enstrophy), Charney (1971) showed that the only possibility is an inverse cascade of total energy.

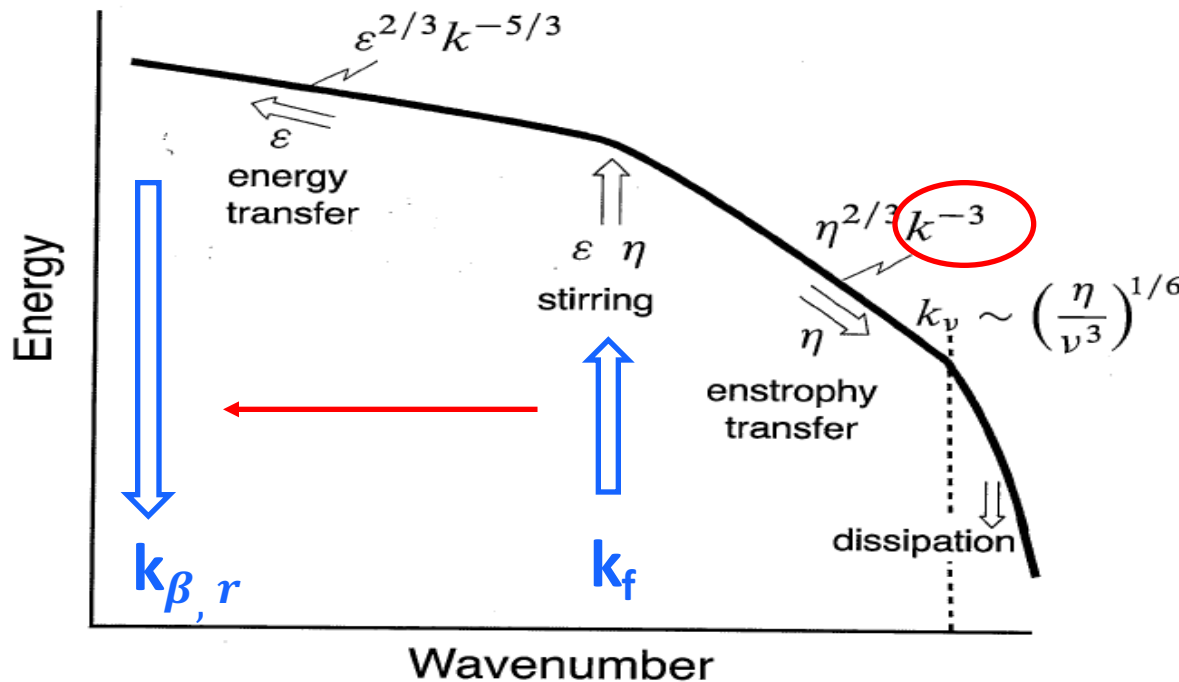
This emphasizes a formal analogy with the Kraichnan arguments for 2-D flows:

**Between  $K_F$  and  $K_\beta$  there is an inertial range with an inverse energy cascade, with**

$$E(\mu) = D_\varepsilon \varepsilon^{2/3} \mu^{-5/3}$$

Evidence of such a  **$K^{-5/3}$  spectrum slope** in the ocean ? ...

# Geostrophic turbulence in the ocean



In the ocean, turbulent geostrophic motions have been considered for a long time to be forced only by the baroclinic instability, whose scales ,  $k_f$  ( $\sim 150 - 200 \text{ km}$ ), are close to the  $\beta$  scale,  $k_{\beta, r}$  ( $\sim 300 \text{ km}$ ). In that case, only a  $k^{-3}$  spectrum slope is expected. [Hua & Haidvogel'86, McWilliams'89, Smith & Vallis'02, Vallis'06]

## Inertial range for the inverse energy cascade

But evidence of such a  **$K^{-5/3}$  spectrum slope** over a large scale range has been recently found in several high resolution numerical simulations.  
[Roullet et al. JPO'12, Sasaki et al. NC'15, Callies et al. JFM'16]

These simulations highlight the existence of source of KE at small scales, larger  $K_F$ , and therefore forcing scales much different from dispersive and removal scales ( $K_{\beta,r}$ ).

**This  $K^{-5/3}$  spectrum slope has been found to be associated with a 3-D inverse KE cascade.**

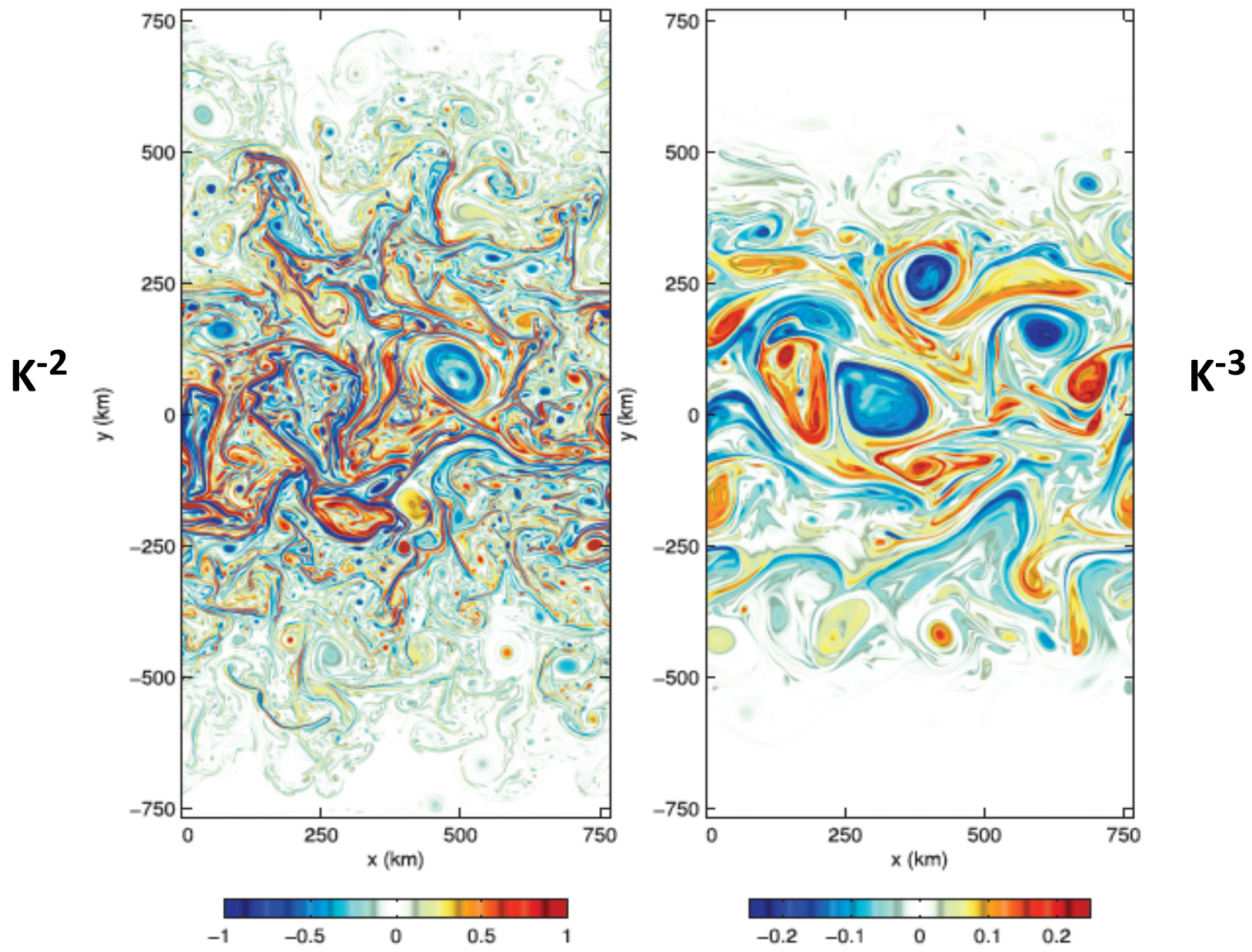


FIG. 5. Surface vorticity snapshot ( $\zeta/f$ ) at the statistical steady state for (left) the Charney case and (right) the Phillips case.

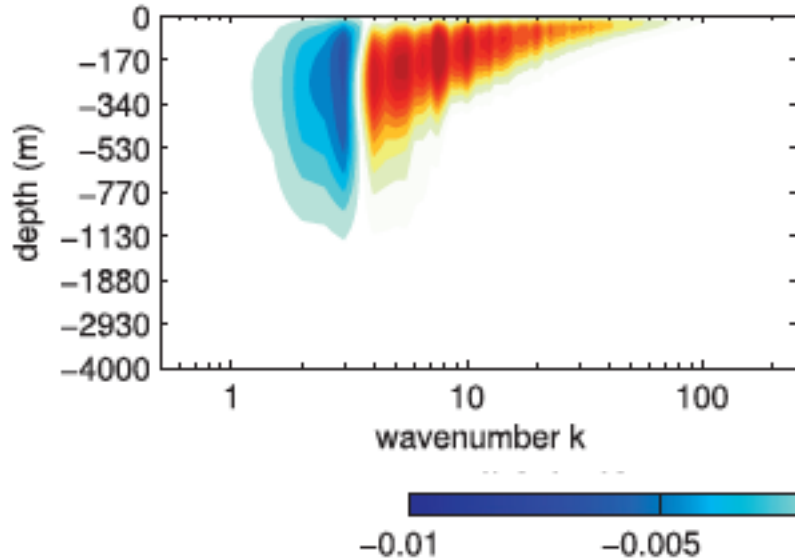
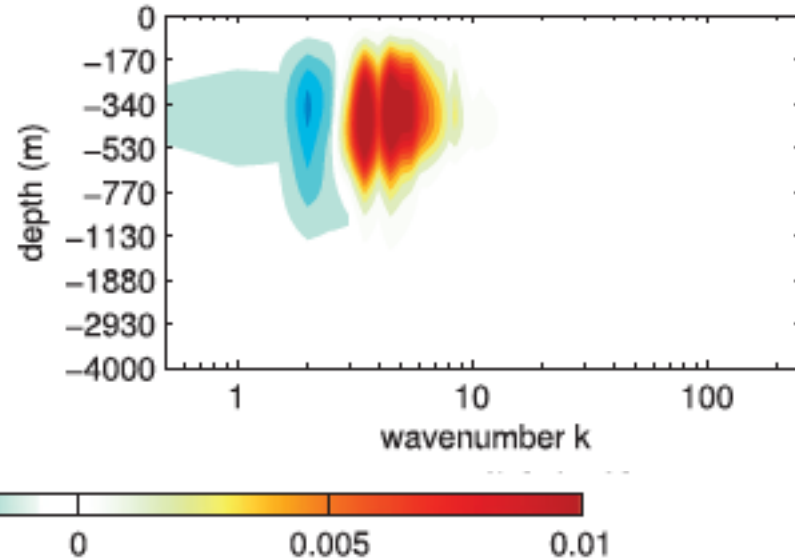
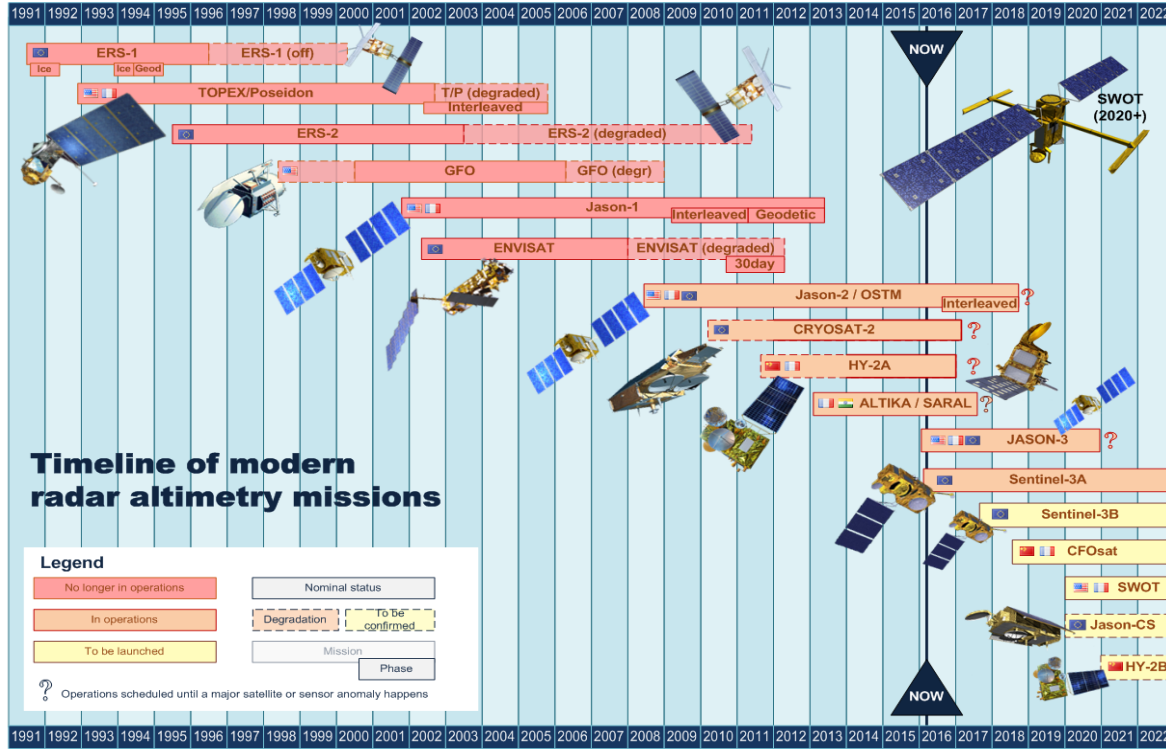
$\kappa^2$  $\kappa^3$ 

FIG. 8. (top) Conversion term  $C = \langle w, b \rangle$  and (bottom) divergence of the vertical energy flux  $\partial_z(w, \psi)$  for (left) the Charney case and (right) the Phillips case. Terms are multiplied by the wavenumber  $k$  to compensate for the logarithmic shrinking. The horizontal resolution is 512 ( $\Delta x = 1.5$  km).

**These results point to the existence of a source of KE at small scales in the ocean, a source that was totally ignored so far.**

**This small-scale KE feeds up larger eddies and larger scales and therefore affects the ocean dynamics.**



**The future satellite missions, and particular the altimeter and SAR missions, should allow to much better capture this ocean dynamics involving small scales and their impact on larger scales.**